Ca^{2+}-Sequestering Smooth Endoplasmic Reticulum in an Invertebrate Photoreceptor. II. Its Properties as Revealed by Microphotometric Measurements

BERND WALZ
Abteilung für Vergleichende Neurobiologie, Universität Ulm, Federal Republic of Germany

ABSTRACT Microphotometric measurements are used to investigate the functional properties of Ca^{2+}-sequestering smooth endoplasmic reticulum (SER) in leech photoreceptors. 10–30 intact cells are mounted in a perfusion chamber, placed between crossed polarizers in a microphotometer, and permeabilized by saponin treatment. Subsequent perfusion with solutions containing Ca^{2+}, MgATP, and oxalate leads to Ca uptake by SER. When the solubility product of Ca-oxalate is exceeded in the SER, birefringent Ca-oxalate precipitates form in the cisternae, leading to a large increase in the optical signal recorded from the preparation. The rate of increase in light intensity is used to measure the rate of Ca uptake.

Ca uptake rate is linear with time over much of its course, can be switched on/off by the addition/withdrawal of Ca^{2+}, ATP, or oxalate to/from the medium, and is inhibited by mersalyl and tetracaine. The Ca uptake mechanism has a high specificity for MgATP ($K_{M,MgATP}$ is ~0.8 mM). Uptake rates observed with dATP, GTP, UTP, ITP, and CTP are only 20–30% of the rate measured in ATP. The Ca pump has a high affinity for Ca^{2+} ions: the threshold for activation of the pump is $\sim 5 \times 10^{-8}$ M, the apparent $K_{M,Ca}$ is $\sim 4 \times 10^{-7}$ M. When Na^+ or Li^+ is substituted for K^+, Ca uptake rate is decreased by 40–50%.

The results show that the Ca^{2+}-sequestering SER in leech photoreceptors shares some basic properties with skeletal muscle sarcoplasmic reticulum and supports the idea that certain subregions of the SER in invertebrate photoreceptors function as effective Ca^{2+} sinks/buffers close to the plasmalemma.

Direct evidence from measurements with Ca^{2+} indicators (6, 8, 9, 26) and Ca^{2+}-sensitive microelectrodes (6), as well as indirect evidence from electrophysiological experiments (see, for example, references 1, 15, 24, 25, 35), suggest that the free calcium concentration (Ca_{in}^{2+}) in the cytosol of photoreceptor cells of invertebrates increases upon illumination. Several laboratories have shown that this light-induced increase of Ca_{in}^{2+} modulates the adaptational state of the cells (see reference 7 for review), a Ca^{2+}-dependent potassium conductance (see, for example, reference 17, 18, 38), and mediates the light-induced pigment granule migration in fly photoreceptors (22).

We have very little direct information about the structures and mechanisms which regulate Ca_{in}^{2+} in invertebrate photoreceptor cells. This means that we do not know the capacities or relative contributions of the plasma membrane, endoplasmic reticulum (ER), mitochondria, and Ca^{2+} binding macromolecules to the regulation of Ca_{in}^{2+} (see reference 10 for review) nor is the influence of light (if any) on these Ca^{2+}-buffering structures understood.

In two preceding papers (43, 46) it was demonstrated, using cytochemical methods, that in leech photoreceptors defined subregions of the smooth endoplasmic reticulum (SER) accumulate Ca^{2+} in an ATP-dependent uptake process. This was shown by incubating saponin-permeabilized cells in a loading medium containing Ca^{2+}, MgATP, and oxalate to stimulate Ca^{2+} sequestration by subcellular organelles. The products of the active Ca uptake are Ca-oxalate precipitates located exclusively within several defined (46) elements of the SER.

Although this method provided valuable information about the nature and topography of the intracellular Ca^{2+} sequestration sites, it is not suited to investigations of either the kinetic properties of the active Ca^{2+} uptake or of factors that influence this process. However, the aim of this study was the investigation of some kinetic aspects of the Ca-uptake mechanism.

THE JOURNAL OF CELL BIOLOGY · VOLUME 93 JUNE 1982 849-859

Therefore, a new microphotometric method is adopted to measure the rate of Ca uptake into the Ca^{2+}-sequestering SER of leech photoreceptors.

The results of these measurements show that the Ca^{2+}-sequestering SER has a very high affinity for Ca^{2+} and shares several basic properties with Ca^{2+}-sequestering SER from other cell types which have been investigated by a completely different method.

The accompanying article (43) and the present article lend strong support to the idea that certain subregions of the SER in invertebrate photoreceptor cells are important in the regulation of Ca_{in}^{2+} in the immediate vicinity of the plasma membrane of these excitable cells.

Preliminary reports of some of the results have already been published in abstract form (44, 45).

MATERIALS AND METHODS

Animals and Chemicals

Hirudo medicinalis was obtained from commercial dealers. The animals were kept in aerated aquaria at 16°C, illuminated by fluorescent light in a 12-h light/12-h dark cycle.

Saponin and EGTA (ethyleneglycol-bis-(β-aminoethyl ether)*N,N*-tetraacetic acid) were obtained from the Sigma Chemical Company (St. Louis, MO). ATP·Na_2 and GTP·Na_2 were purchased from E. Merck (Darmstadt, Germany), desoxyATP·Na_2, UTP·Na_2, ITP·Na_2, and CTP·Na_2 from Boehringer (Mannheim, Germany).

Preparation and Mounting of the Photoreceptor Cells

Single pigmented eye cups were excised from the dorsal side of the anterior end of the leech and freed from excess tissue in physiological saline. Subsequently, a transverse section, ~200 μm in thickness, was sliced from the slightly elongated eye cup. This preparation contains about 10–30 photoreceptor cells, depending on the thickness of the slice and the eye size.

Light Recordings (Fig. 1)

The eye slice was mounted in a shallow, uncovered, glass-bottomed perfusion chamber on the rotatable stage of a Zeiss photomicroscope (PHOMI III). For the measurements, a 25-power water-immersion-objective (Zeiss, Neofluar, N.A. 0.8, not strain-free) was used.

A DC-powered 12-V, 100-W halogen lamp served as the light source. The light passed through a heat-absorbing filter and a plane polarizer, and was then concentrated on the specimen with a strain-free condensor (Zeiss, oil-immersion-condensor, N.A. 1.4). Using the illumination field diaphragm, the field of measurement was restricted to the photoreceptor cells within the eye slice. Stray light was minimized by closing the aperture diaphragm of the condensor.

The light transmitted by a second polarizer (analyzer, aligned in the crossed position) above the photoreceptor cells was measured by the light detector, an RCA 8575 photomultiplier tube (PM), mounted on the microscope. An additional iris diaphragm in front of the cathode allowed the regulation of light reaching the cathode. The PM was operated with the anode at virtual ground. Voltages (HV) applied to the dynode chain varied between 700 and 900 V. The anode current of the PM, converted to a voltage signal, was displayed on an oscilloscope (OS) and recorded on a chart recorder (R). The optical signal recorded from the photoreceptor cells is presented as anode current.

For investigations of the optical properties of blank and loaded preparations, a λ/4 retardation plate (PV 140, E. Käsemann, Oberaudorf, Germany) was introduced into the light path between the preparation and a rotatable analyzer to allow the introduction of variable amounts of retardation, according to the method of Sénarmont-Friedel (see reference 3 for methodological details). These experiments were performed at a wavelength of light of 542 nm and documented microphotographically.

Experimental Protocol

The experiments start by substituting lysis medium for the physiological saline in the perfusion chamber. Preliminary experiments showed that a period of 5–10 min in the lysis medium containing 500 μg/ml saponin is sufficient to permeabilize all cells within the preparation. At the end of the lysis period, the shutter of the PM is opened to measure the light intensity coming from the preparation and passing the analyzer. Then, the lysis medium is replaced by the appropriate loading medium (see results and figure legends for details). All test solutions are vigorously stirred during the whole experiment by means of a small rotating propeller.

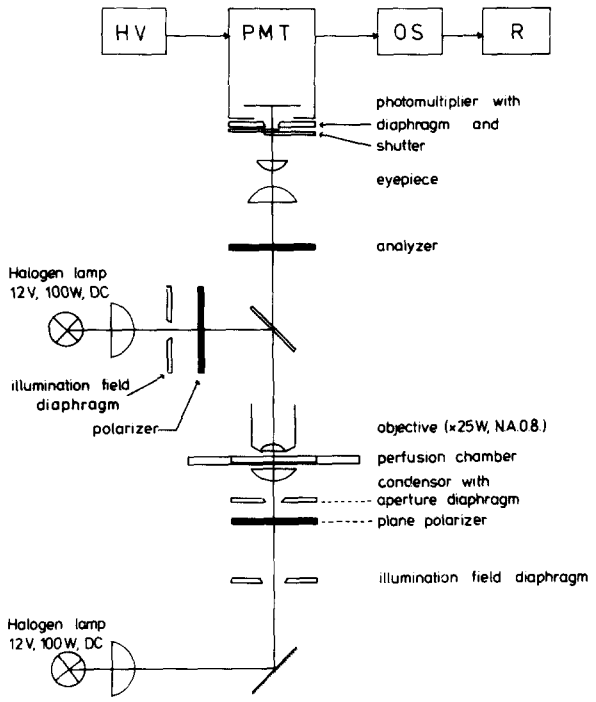

FIGURE 1 Schematic diagram of the microphotometer used for measurements of the birefringence of photoreceptor cells. *PMT*, photomultiplier tube; *HV*, high-voltage power supply; *OS*, oscilloscope; *R*, strip chart recorder. The measurements in the present study were done by transmission polarization microscopy. The light path for incident illumination is included because similar optical recordings are possible by measuring the light which is reflected and depolarized by the preparation.

Tests for Linearity of the Method

The aim of the present study was to measure microphotometrically the rate of the ATP-dependent formation of Ca-oxalate and to use the rate of changes in the optical signal as a measure of e.g. the rate of Ca uptake. To demonstrate that (*a*) the size of the optical signal is a linear function of the amount of Ca-oxalate in the field of measurement (in the preparation), and that (*b*) a linear function exists between the rate of rise in the optical signal ($\Delta I/\Delta t$) and the various rates of Ca^{2+} entry ($\Delta c_{Ca}/\Delta t$) into the compartment in which its precipitation as Ca-oxalate occurs ($\Delta c_{Ca\text{-}oxalate}/\Delta t$), it was shown, for a given oxalate concentration, that

$$\frac{\Delta c_{Ca}}{\Delta t}\left(\frac{\Delta c_{Ca\text{-}oxalate}}{\Delta t}\right) \sim \frac{\Delta I}{\Delta t}.$$

In these tests the setting of the equipment was the same as for the actual experiments but without a preparation in the light path. The microscopic dimension of the eye slice prohibits these points being tested in the tissue. Further experimental details are given in the legends of Fig. 2 *a*, *b*. In both types of experiments the size and the density of the Ca-oxalate precipitates produced in the field of measurement mimic fairly well these two parameters in the preparation.

The results presented in Fig. 2 *a*, *b* show a linearity between the optical signal and $c_{Ca\text{-}oxalate}$ and $\frac{\Delta c_{Ca}}{\Delta t}$, respectively, over a large range of Ca-oxalate concentrations (Fig. 2 *a*) and a large range of rates of Ca^{2+} concentration changes (Fig. 2 *b*).

Thus, if Ca-oxalate formation in the SER cisternae does not follow completely different rules, the microphotometric method used appears adequate for monitoring the chemistry/dynamics of Ca uptake.

Solutions

The *Hirudo* physiological saline had the following composition (mM): NaCl 113.5, KCl 4.3, $CaCl_2$ 1.8 maleic acid 10.0, and Tris (hydroxymethyl) aminomethane 10.0. The pH was adjusted with NaOH to 7.4.

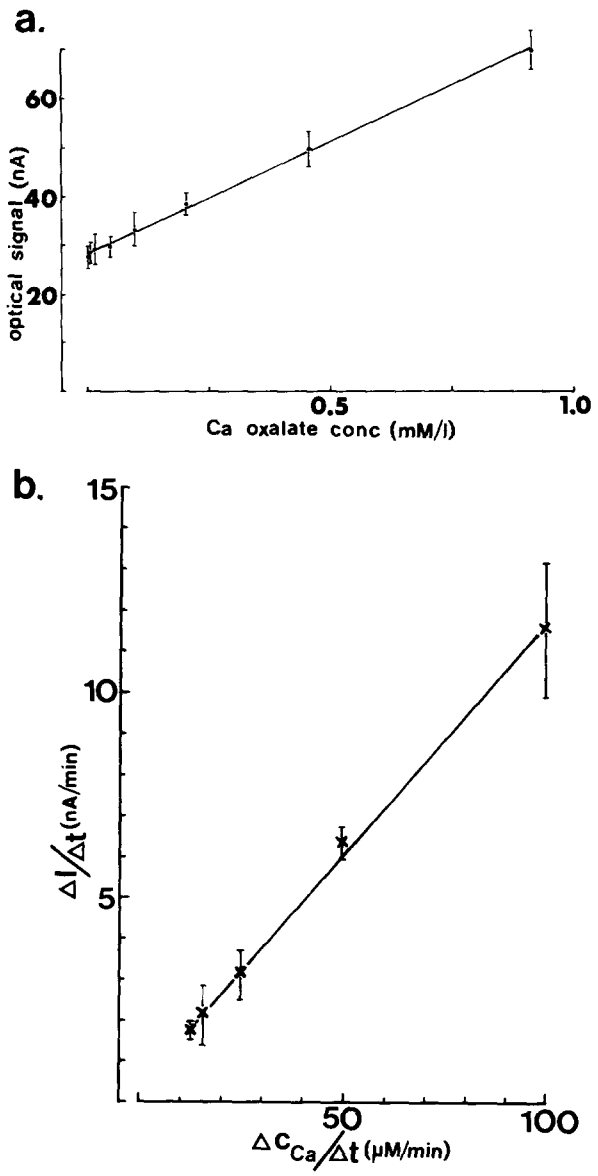

FIGURE 2 Experimental tests for linearity of the microphotometric method. The experimental arrangement for the in vitro measurements is identical to that used in the *in situ* accumulation experiments. (*a*) Optical signal as a function of the "amount" of Ca-oxalate in the field of measurement. A Ca-oxalate stock solution (0.83 mM/liter) was prepared by adding a known amount of a solution containing $CaCl_2$ (KCl 100 mM, Imidazol/HCl 20 mM, $CaCl_2$ 5 mM, pH 7.0) to a solution containing 75 mM KCl, 25 mM K-oxalate, 20 mM Imidazol/HCl, pH 7.0. Part of the resulting Ca-oxalate suspension was filtered, and the filtrate used to prepare a sequence of test solutions by diluting the stock solution. The figure demonstrates that linearity exists between the "amount" of Ca-oxalate in the light path and the recorded optical signal. The line is drawn by a least-squares fit: $y = 49.97 + 27.96$ ($r^2 = 1.0$). Each point gives the mean value (±SD) from 12 determinations. (*b*) Rate of rise in the optical signal ($\Delta I/\Delta t$) as a function of the rate of rise of Ca^{2+} concentration ($\Delta c_{Ca}/\Delta t$) in the perfusion chamber. The chamber contained 2 ml of a solution consisting of 75 mM KCl, 25 mM K-oxalate, and 20 mM Imidazol/HCl, pH 7.0. This solution was vigorously stirred and titrated with a test solution (KCl 100 mM, $CaCl_2$ 5 mM, Imidazol/HCl 20 mM, pH 7.0) at a sequence of constant rates. $\Delta I/\Delta t$ was plotted as a function of $\Delta c_{Ca}/\Delta t$. Each symbol gives the mean ± SD from four determinations. The line was fitted by eye. The figure illustrates that a linear function exists between $\Delta I/\Delta t$ and $\Delta c_{Ca}/\Delta t$. Both experiments provide evidence that the optical signal varies linearly with the formation of Ca-oxalate.

The lysis medium contained (mM): KCl 100, $MgCl_2$ 5, ATP·Na_2 5, K_2EGTA 2, Imidazol/HCl 20, and sucrose 40. The pH was adjusted to 7.0 with KOH. 500 μg/ml saponin were added immediately before use and dissolved by sonication.

The standard loading medium had the following composition (mM): KCl 75, K-oxalate 25, $MgCl_2$, 5, ATP·Na_2 5, K_2EGTA 1, CaEGTA 4, Imidazol/HCl 20, and sucrose 40. The pH of this medium was adjusted to 7.0 with KOH. The concentration of free Ca^{2+} in this solution was calculated (see below) to be ≅ 8.5 × 10^{-7} M. The composition of each particular loading medium is described in the respective figure legend and in the results. In those experiments in which ionized Ca^{2+} was to be changed in the loading media, the various free Ca^{2+} concentrations were adjusted by changing the ratio of CaEGTA to K_2EGTA and keeping total EGTA constant at 5 mM.

Experimental solutions were prepared freshly every day from 1 M or 0.1 M stock solutions of the various components. The stock solution of K_2EGTA (Na_2EGTA) was prepared from KCl (NaCl), H_4EGTA, and KOH (NaOH) and the stock solution of CaEGTA from $CaCO_3$ (or $CaCl_2$), H_4EGTA, and KOH. The pH of these solutions was adjusted with KOH or NaOH to 7.0.

Calculation of Ca^{2+}_{free}, Mg^{2+}_{free}, and $MgATP^{2-}_{free}$

The free calcium concentrations in the loading media were buffered with EGTA. The actual concentrations of Ca^{2+}_{free}, Mg^{2+}_{free}, and $MgATP^{2-}_{free}$ depend on the total amounts of Ca_{total}, Mg_{total}, $EGTA_{total}$, and ATP_{total}, and on the apparent association constants K_{CaEGTA}, K_{MgEGTA}, K_{CaATP}, and K_{MgATP}.

Calculations of the concentrations of free ions (Ca^{2+}_{free}, Mg^{2+}_{free}), free ligands ($EGTA_{free}$, ATP_{free}) and ion-ligand-complexes ($CaEGTA_{free}$, $MgEGTA_{free}$, $CaATP_{free}$, $MgATP_{free}$) were made by programming a PDP 11 computer to solve the following set of equations by an iterative procedure (37):

$$K_{CaEGTA} = \frac{a}{(Ca_{total} - a - d)(EGTA_{total} - a - b)} \quad \text{Eq. 1}$$

$$K_{MgEGTA} = \frac{b}{(Mg_{total} - b - c)(EGTA_{total} - a - b)} \quad \text{Eq. 2}$$

$$K_{MgATP} = \frac{c}{(Mg_{total} - b - c)(ATP_{total} - c - d)} \quad \text{Eq. 3}$$

$$K_{CaATP} = \frac{d}{(Ca_{total} - a - d)(ATP_{total} - c - d)} \quad \text{Eq. 4}$$

where $a = CaEGTA_{free}$, $b = MgEGTA_{free}$, $c = MgATP_{free}$, and $d = CaATP_{free}$. Furthermore, $EGTA_{free} = EGTA_{total} - a - b$. $ATP_{free} = ATP_{total} - c - d$. $Ca^{2+}_{free} = Ca_{total} - a - d$. $Mg^{2+}_{free} = Mg_{total} - b - c$.

The calculations started by solving Eq. 1 for a setting $b = 0$ and $d = 0$. The calculated value for a is substituted into Eq. 2 which is solved for b, setting $c = 0$. Eq. 3 is solved for c with the calculated value of b, setting $d = 0$. For the calculation of d, a and c are substituted into Eq. 4.

Then, the calculated values for b and d are substituted into Eq. 1 to calculate an updated value for a, and so on. The calculations were stopped when subsequent values for a did not differ by $>10^{-9}$ M. The following apparent association constants were used for the calculations: $K_{CaEGTA} = 4.83 \times 10^6$ M^{-1}, $K_{MgEGTA} = 40$ M^{-1} (calculated from the absolute constants for pH 7.0 according to reference 36), $K_{MgATP} = 5 \times 10^3$ M^{-1}, $K_{CaATP} = 1.14 \times 10^4$ M^{-1} (from reference 33).

RESULTS

Calcium Accumulation in Photoreceptor Cells

The fundamental observation for the microphotometric measurements in the present study is demonstrated in Fig. 3. Fig. 3 *a–c* shows photoreceptor cells of the leech between crossed polarizers at the end of a typical accumulation experiment. The preparation was treated for 10 min with the lysis medium to break down the plasmalemmal permeability barrier and then was incubated for ~30 min in the standard loading medium. The arrows label Ca-oxalate deposits within the plane of focus. These stand out brightly against a moderately dark background. Precipitates located above and below the plane of focus, as well as the preparation itself, contribute to a diffuse background brightness. As a comparison of Fig. 3 *d*, *e*, and *f* shows, the precipitates outline the "vacuole" of the photoreceptor cells. Two preceding cytochemical studies (43, 46) revealed that these prominent precipitates are located within the elaborate submicrovillar cisternae, the most prominent Ca-sequestering subregion of the SER.

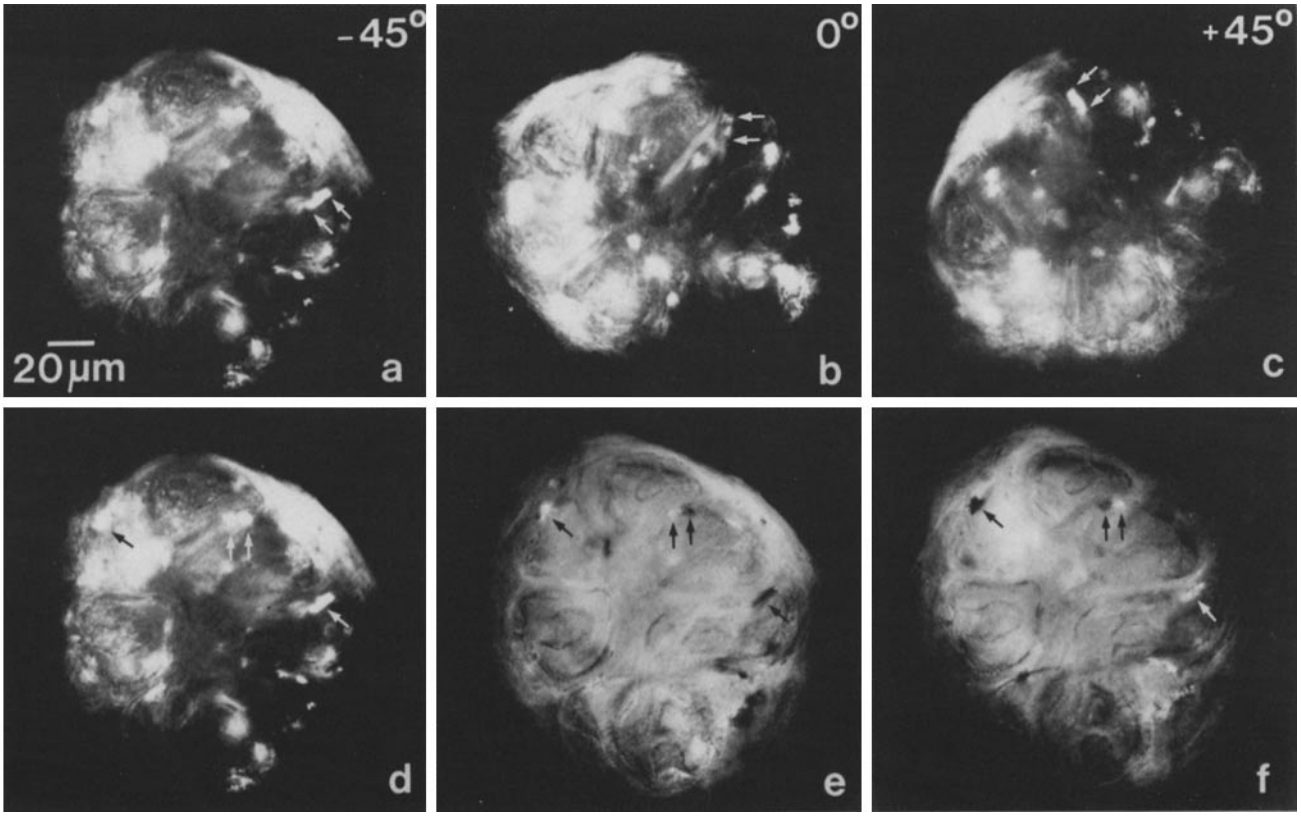

FIGURE 3 Eye slice as viewed in the polarizing microscope after the SER has been loaded with Ca-oxalate. Since the illumination field diaphragm has been closed, the camera (and the photomultiplier) "sees" only the photoreceptor cells located in the center of the slice. The arrows label some sites where Ca-oxalate deposits have been formed in the plane of focus. The sequence of micrographs documents the results of two optical tests for birefringence. (*a–c*) Pattern of Ca-oxalate deposits on rotating the object on the stage over an arc of 90°. The individual deposit labeled by the pair of arrows shows maximum brightness at ±45°, and extinction at 0°. (*d–f*) Effect of introducing variable amounts of compensation on the pattern of Ca-oxalate deposits. (*d*) uncompensated, (e) with −66 nm, and (*f*) −427 nm of retardation introduced by the compensator at a wavelength of light of 542 nm. Note the contrast reversal of the deposits (arrows) upon compensation. The deposits appear dark when the net phase shift at the analyzer is zero.

Optical Properties of the Preparation

The Ca-oxalate deposits in the loaded preparation shine brightly when observed between crossed polarizers. The brightness of the deposits arises primarily from the birefringent nature of Ca-oxalate and is most likely not due to light scattering: (*a*) On rotation on the stage, the preparation shows a pattern of brightly shining deposits which varies with specimen rotation. Observing an individual deposit (Fig. 3 *a–c*), it can be seen that the particle shows four azimuths of extinction and four of brightness when rotated through 360°. This test also demonstrates that the Ca-oxalate deposits in the preparation show random orientation. Some deposits consist of microscopic particles with their axis forming an angle of ±45° with the azimuth of the polarizers, regardless of the direction of orientation of the stage. This is also evident when a first-order retardation plate is introduced between preparation and analyzer. Individual deposits shine yellow, others blue. These deposits reverse their color when the stage is rotated over an arc of 90°. (*b*) All brightly shining deposits can be darkened by compensation (quarterwave plate method according to Sénarmont-Friedel; see reference 3 for details). However, different particles have different retardations, i.e. at no compensator setting is it possible to darken all deposits simultaneously (Fig. 3 *d–f*). This is again due to the fact that the accumulation

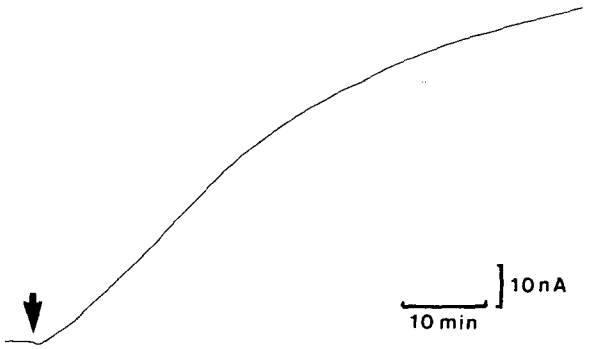

FIGURE 4 Continuous recording of the time-course of the birefringence signal. The arrow indicates, when the lysis medium was replaced by the standard loading medium. After a small negative deflection, the optical signal rises due to the formation of birefringent Ca-oxalate precipitates in the SER of the cells.

experiments produce a large number of small anisotropic particles in the various cells and cisternae at random orientation.

None of these tests for birefringence would be positive if the brightness of the deposits arose from light scattering. On the basis of these observations, the optical signal recorded from the preparations upon their loading with Ca-oxalate is called a birefringence signal (although a contribution of some light

scattering to the optical signal can not be completely ruled out).

Time Courses and General Requirements for the Ca-Oxalate Formation

Fig. 4 shows one example of the time course of the Ca-oxalate formation. After superfusion of the preparation with the standard loading medium (arrow) there is a brief negative deflection followed by a large increase in the optical signal due to an increasing depolarization of the polarized light caused by the formation of birefringent Ca-oxalate precipitates within the SER.

The brief (<2 min) negative deflection is always observed immediately after the loading medium is substituted for the lysis medium (see Figs. 5 (*a*, *b*), 7, 12, and 14). The reasons for this transient "darkening" of the preparation were not systematically investigated because this negative response did not interfere with the subsequent recording of the optical signal specific for the formation of Ca-oxalate.

The optical signal in Fig. 4 increases linearly for ~20 min and only then slowly saturates. The duration of the linear phase varies with the preparation and the type of experiment. In other experiments the linear phase lasted for up to 1 h.

Fig. 5 *a* shows that the increase in the optical signal comes to an immediate halt when the precipitating anion oxalate is withdrawn from the loading medium. In the oxalate-deprived loading medium the optical signal starts to decrease. Since in the SER cisternae the Ca-oxalate precipitates are in equilibrium with Ca^{2+}_{free} and $oxalate^{2-}_{free}$ (their concentrations being buffered at a value set by the Ca-oxalate solubility product), imposing a concentration gradient for $oxalate^{2-}$ across the SER membrane, by eliminating this ion from the medium, will produce an efflux of $oxalate^{2-}$ from the SER. This results in the observed decomposition of the intracisternal Ca-oxalate precipitates.

An important result is illustrated in Fig. 5 *b*. The rise in the optical signal is immediately abolished when ATP is withdrawn from the loading medium. The rise in the optical signal is therefore not due to some kind of unspecific and/or passive Ca-oxalate formation in the SER but reflects an ATP-dependent Ca^{2+}-uptake process.

The results so far reported also show that the use of saponin to permeabilize the plasma membrane of the cells leaves the SER membrane sufficiently intact, not impairing the ability of the SER to take up Ca^{2+}. The necessity for an intact SER membrane is shown in experiments (no figure) in which 0.5% Triton X-100 was added to the lysis medium. Treatment with this substance completely prevents the formation of Ca-oxalate precipitates during subsequent superfusion with the standard loading medium.

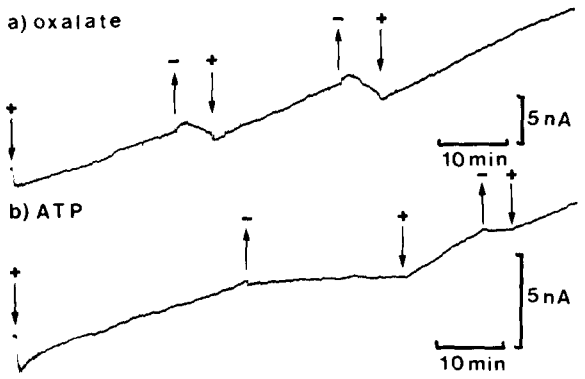

FIGURE 5 Two original recordings demonstrating the requirement for a precipitating anion (*a*) and an energy-supplying substrate (b) to initiate and maintain a rise in the optical signal. Recording starts when the preparation was superfused with the complete standard loading medium (+). (−) indicates when the standard loading medium is replaced by oxalate and ATP-free medium, respectively.

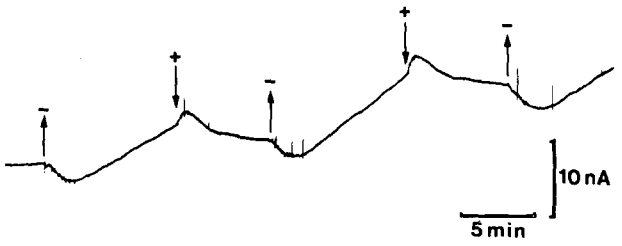

FIGURE 6 Reversible inhibition of the Ca uptake by tetracaine (10 mM). Recording starts with the replacement of the lysis medium by drug-free (−) standard loading medium which is twice replaced by the tetracaine-containing (+) standard loading medium.

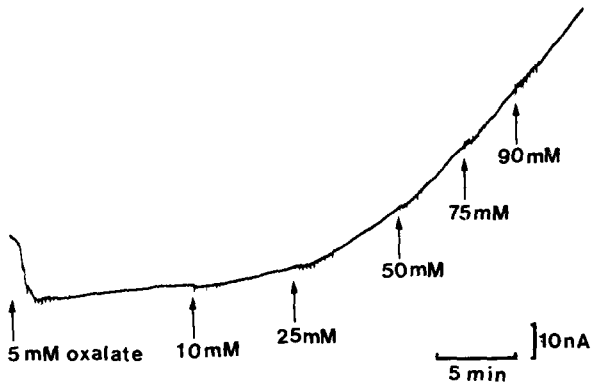

FIGURE 7 Effects of increasing oxalate concentrations on the Ca-uptake rate. The experiment was performed with loading media containing only 5×10^{-7} M Ca^{2+}_{free}. While 5 mM oxalate already led to a measurable rise in the optical signal, raising the oxalate concentration above 50 mM leads only to a small additional increase of the Ca-uptake rate.

Two substances that have been shown (20, 21, 30) to inhibit active Ca uptake into fragmented sarcoplasmic reticulum and into microsomal preparations from other cell types (e.g., reference 4) were tested for their effects on the ATP-dependent Ca uptake into the SER of leech photoreceptors: 1 mM of the SH reagent mersalyl, as well as 10 mM of the local anesthetic tetracaine (Fig. 6), inhibits active Ca uptake. Fig. 6 also shows that the effect of tetracaine is reversible. The slow decrease in the optical signal upon tetracaine addition indicates that Ca^{2+} is released from the SER, leading to a slow degradation of Ca-oxalate precipitates.

Effect of Oxalate Concentration on Ca-uptake Rate

Fig. 7 shows the optical signal recorded from a preparation which was incubated in a sequence of loading media with increasing oxalate concentrations ($Ca^{2+}_{free} \cong 5 \times 10^{-7}$ M). The figure illustrates that the measurable Ca uptake proceeds slowly in a loading medium containing only 5 mM oxalate but that the rate of uptake increases with increasing oxalate concentration (up to 50 mM oxalate) in the loading medium. A further

increase of the oxalate concentration enhanced the Ca-uptake rate in the illustrated example to only a small degree.

Fig. 8 summarizes the results of five measurements of this type. This figure was obtained by normalizing the rates at lower oxalate concentrations to the rate in 90 mM oxalate. The relative rate of Ca uptake does not saturate completely in the concentration range tested. Higher oxalate concentrations were not tested, as Ca-oxalate precipitates spontaneously in loading media containing 5×10^{-7} M Ca^{2+}_{free} and oxalate concentrations $\geq$100 mM. The relatively high standard deviations indicate a high variability among the preparations against variations of the oxalate concentration. An oxalate concentration of 25 mM was selected for the standard loading medium.

Nucleotide and Mg^{2+} Requirements for the Active Uptake of Ca^{2+}

As already shown (Fig. 5*b*) the active Ca uptake, as measured by the rise in the optical signal recorded from the cells, is completely abolished when ATP is withdrawn from the loading medium. Experiments were carried out to determine the effectiveness of nucleotide triphosphates (NTP's) other than ATP in promoting the active uptake of Ca^{2+} (the concentrations used were NTP = $MgCl_2$ = 5 mM).

A baseline rate of Ca uptake was determined by recording from cells in the standard loading medium (+ ATP). When the optical signal rose at a constant rate for several minutes, this loading medium was replaced by another in which the ATP had been replaced by some other NTP. Recording was continued until the rate of uptake in this new medium remained constant for several minutes, after which the preparation was returned to the original solution. The rates of Ca uptake in the various test media were expressed relative to the mean of the control rates in ATP-containing media. Fig. 9 shows the high specificity of the Ca-uptake mechanism for ATP. The Ca-uptake rate promoted by dATP, GTP, UTP, ITP, and CTP is only 20–30% of the rate measured in ATP.

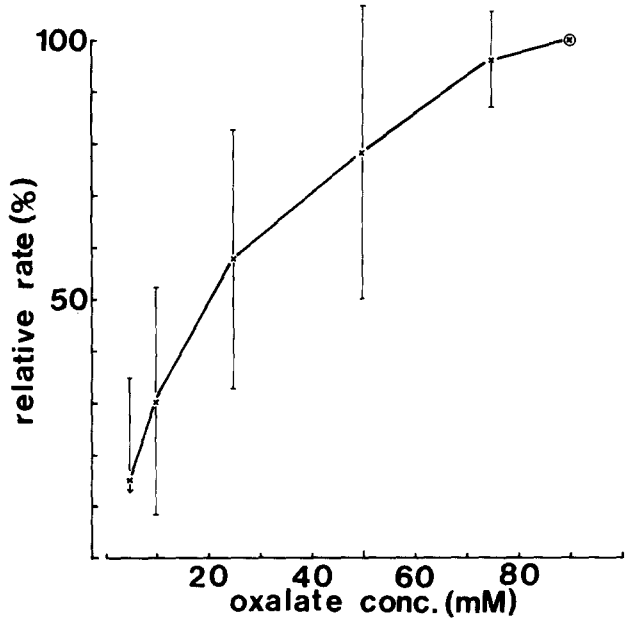

FIGURE 8 Oxalate concentration dependence of Ca-uptake rate. The graph shows mean values (±SD) from the results of five measurements of the kind illustrated in Fig. 7. The rates in the lower oxalate concentrations in each experiment were normalized to the rate in 90 mM oxalate.

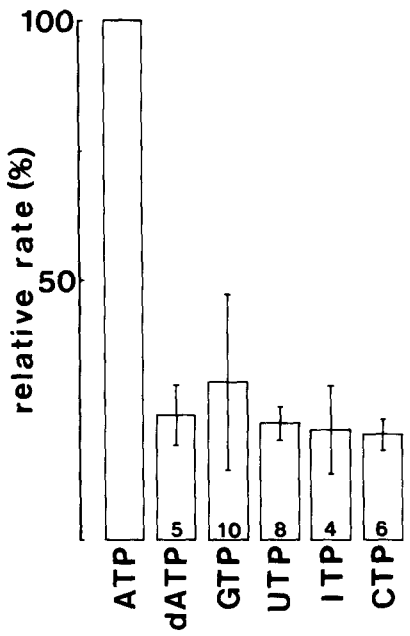

FIGURE 9 Effects of various nucleotide triphosphates on the Ca-uptake rate. The number of experiments is given at the base of each bar. Each bar gives the mean value (±SD) from experiments in which the rate of Ca uptake was in each case normalized to the rate in the ATP-containing standard loading medium.

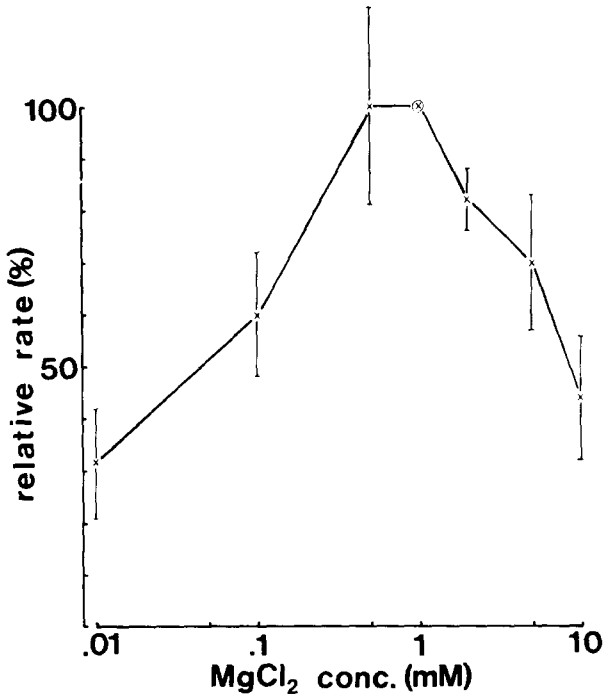

FIGURE 10 The effect of $MgCl_2$ concentration on Ca-uptake rate. Each symbol gives the mean value (±SD) from three to seven experiments. In these experiments each preparation was superfused with standard loading media (Ca^{2+}_{free} = 8.5 × 10^{-7} M; ATP_{total} = 5 mM) containing increasing concentrations of $MgCl_2$. Ca-uptake rates were normalized to the rate in 1 mM $MgCl_2$.

For measurements of the effects of various Mg concentrations on the active Ca uptake, each preparation was successively superfused with loading media containing increasing amounts of $MgCl_2$. The total concentration of ATP in the loading media was kept constant at 5 mM. Fig. 10 presents mean values of data obtained from three to seven determina-

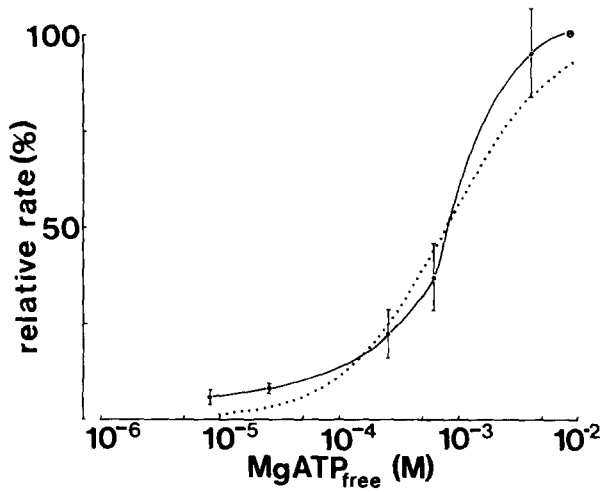

FIGURE 11 The relative rate of Ca uptake as a function of the logarithm of the concentration of $MgATP_{free}$. Each symbol gives the mean value (±SD) from six experiments. For each experiment, the rates at lower $MgATP_{free}$ concentrations were normalized to the rate in 8.6 mM $MgATP_{free}$. The solid curve was drawn by eye through the uptake data. The dotted curve was calculated applying Michaelis-Menten kinetics, according to the equation: $V = V_{max}/[1 + (K_M/Ca^{2+}_{free})]$, setting $K_M = 0.8$ mM.

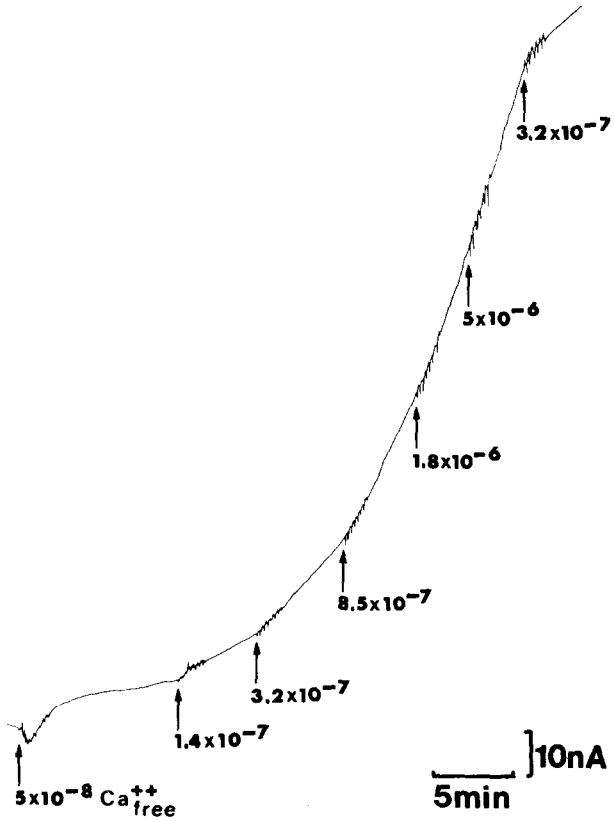

FIGURE 12 Recording from a representative experiment showing the effects of increasing free Ca^{2+} concentrations on the rate of Ca uptake. The preparation was successively superfused with loading media (25 mM oxalate; Mg_{total} = ATP_{total} = 5 mM) containing increasing concentrations of Ca^{2+}_{free}. The recording starts at the time when the lysis medium was replaced by the loading medium with the lowest free Ca^{2+} concentration, which led to a detectable rise in the optical signal. At the end of the experiment a lower Ca^{2+} concentration was again applied as a control.

tions. The rate of uptake at each $MgCl_2$ concentration in a given preparation was normalized to the rate in 1 mM $MgCl_2$. The data show the requirement for Mg^{2+} ions to fully activate the Ca-uptake mechanism. Higher Mg^{2+} concentrations, however, are inhibitory.

Changes in the concentration of Mg_{total} in loading media with constant ATP_{total} produce concomitant changes in Mg^{2+}_{free} and $MgATP_{free}$. If the latter is the true substrate for the transport enzyme, this measurement is ambiguous as to the true effect of Mg^{2+} ions on the active Ca uptake.

In the experiment illustrated in Fig. 11, the effect of various concentrations of $MgATP_{free}$ on the rate of Ca uptake was measured. In this experiment the concentrations of Mg_{total} = ATP_{total} were simultaneously changed between 0.01 mM and 10 mM. This procedure produces changes in $MgATP_{free}$ between 8.3 μM and 8.6 mM, respectively (Fig. 11). In six experiments the rates for each $MgATP_{free}$ concentration were normalized to the highest rate in 8.6 mM $MgATP_{free}$. The measurements show that 8.6 μM $MgATP_{free}$ are sufficient to measurably activate the Ca-uptake mechanism. The relative rates of Ca uptake follow, approximately, Michaelis-Menten-kinetics (dotted curve in Fig. 11) with a K_M value of ~0.8 mM.

Effect of the Ca^{2+} Concentration on the Rate of Ca Uptake

Fig. 12 shows the rise of the optical signal recorded from a preparation which was superfused with loading media containing 25 mM oxalate but increasing concentrations of Ca^{2+}_{free}. The optical signal increases with a slope that depends on the concentration of Ca^{2+}_{free}. Normalizing the rates to the highest rate in 1.8 μM Ca^{2+}_{free} gives a sigmoidal dependency of the relative uptake rate vs. log Ca^{2+}_{free} (Fig. 13). The threshold for

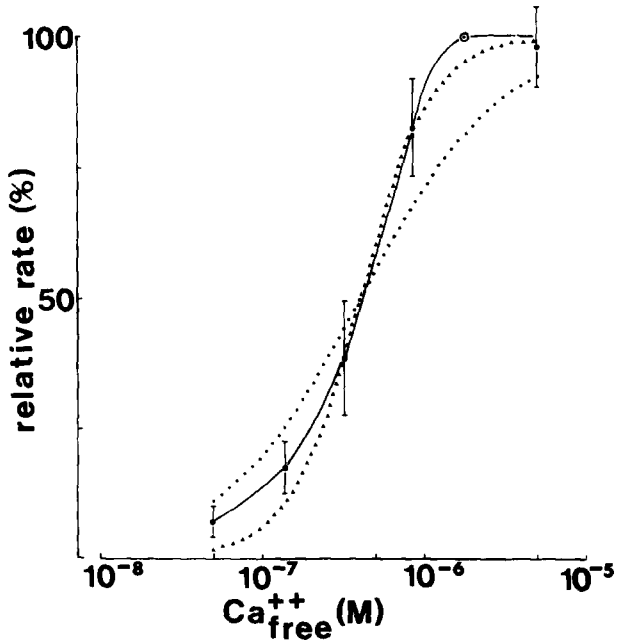

FIGURE 13 The relative rate of Ca^{2+} uptake as a function of the logarithm of the free Ca^{2+} concentration. Each symbol gives the mean value (±SD) from seven experiments of the type illustrated in Fig. 12. For each experiment, the rates were normalized to the rate in 1.8×10^{-6} M Ca^{2+}_{free} (⊙). The solid curve was drawn by eye. The broken curves were calculated according to the equation $V = V_{max}/[1 + (K_M/Ca^{2+}_{free})^n]$, with $n = 1$ (dotted curve; normal Michaelis-Menten kinetics), and $n = 2$ (triangles for the square law relationship), setting $K_M = 0.4$ μM.

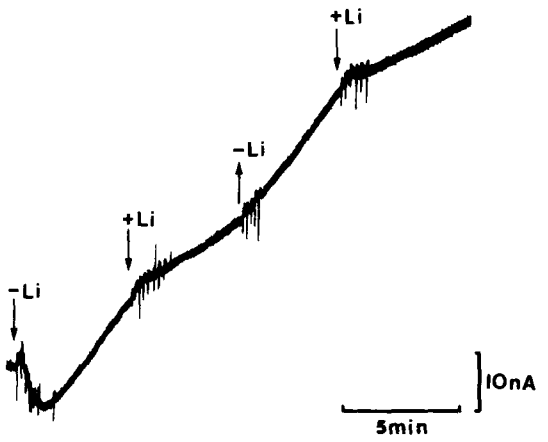

FIGURE 14 The effect of substituting lithium for potassium on the Ca uptake. The recording starts when the lysis medium was replaced by the Li^+-free ($-Li$) standard loading medium. In the Li-containing medium, 100 mM KCl were replaced by 100 mM LiCl (+). Measurements of this type delivered the data for Fig. 15.

the activation of the pump is $\cong 5 \times 10^{-8}$ M, and the Ca-uptake rate is half-saturated at $\cong 4 \times 10^{-7}$ M. The broken curves in Fig. 13 are calculated using the equation $V = V_{max}/[1 + (K_M/Ca^{2+}_{free})^n]$.

In contrast to simple Michaelis-Menten-kinetics ($n = 1$, dotted curve), the square law relationship ($n = 2$, curve labeled with triangles) gives a better fit to the data.

This observation is consistent with data provided by Blaustein et al. (5) for Ca uptake into the nonmitochondrial Ca^{2+} store (SER; see reference 31) in presynaptic nerve terminals. Both the Ca uptake and the ATPase data in that study (5) suggest a stoichiometry of 2 Ca taken up for 1 ATP hydrolyzed on the basis of a Hill coefficient of 1.6 for the kinetic data.

Effect of Monovalent Cations on the Rate of Ca Uptake

Since the photoreceptor cell membranes had been permeabilized, the potassium concentration in the various loading media was chosen to simulate approximately the typical intracellular K^+ concentration. The recording in Fig. 14 shows that the Ca-uptake rate is significantly and reversibly decreased when 100 mM K^+ is replaced by an equimolar amount of Li^+. Complete replacement of K^+ by Na^+ (169 mM), as well as replacement of 100 mM K^+ by Li^+, reduces the rates of Ca uptake to 50–60% of the rate in the standard loading medium (Fig. 15*a*). Fig. 15*b* shows that a rise of Na^+ by only 25 mM reduces the Ca-uptake rate by ~30%. Substituting more Na^+ for K^+ only leads to a small additional inhibition of the Ca-uptake rate.

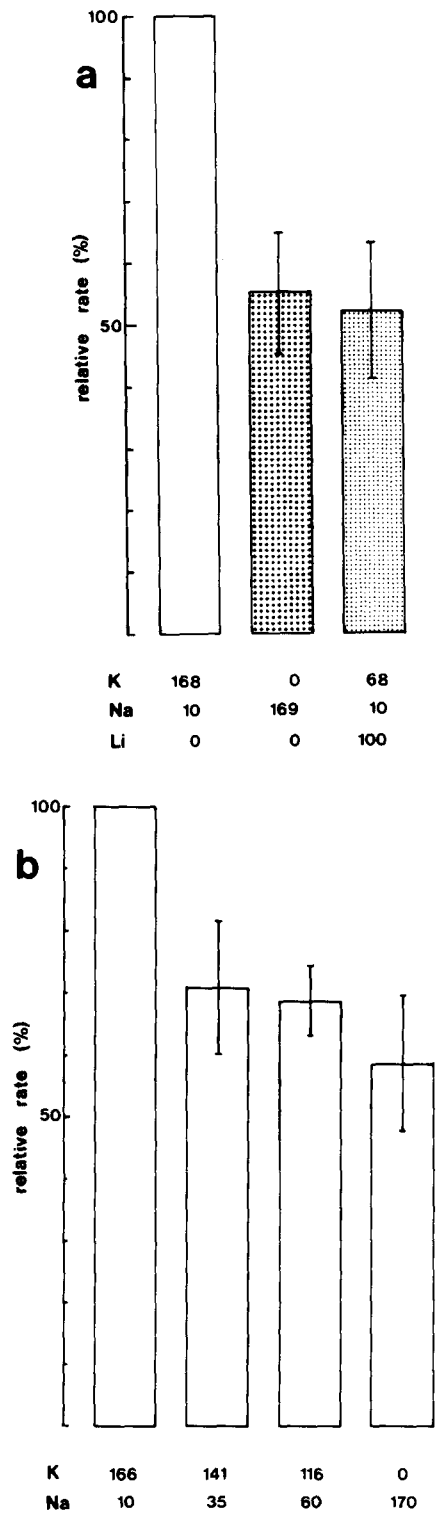

FIGURE 15 The effect of monovalent cations (Na^+, Li^+) on the rate of Ca uptake. Each bar gives the mean value (±SD) from three to twelve determinations. For every experimental condition the rate of Ca uptake was normalized to the rate in the standard loading medium (K^+ 166 or 168 mM, Na^+ 10 mM). (*a*) Effect of Na^+ and Li^+. Substituting K^+ for both ionic species inhibits in the indicated concentrations the uptake rate by 40–50% of the control rate. (*b*) The effect of increasing Na^+/decreasing K^+ concentrations on Ca uptake rate. Note that the uptake rate is already inhibited by ~30% when the sodium/potassium concentration in the loading medium is increased/decreased by only 25 mM.

DISCUSSION

Methodological Aspects

The small size and cellular heterogeneity of the eyes of most invertebrates make it difficult to obtain a pure subcellular (microsomal) fraction of smooth endoplasmic reticulum (SER) from the visual cells. Thus, the Ca^{2+}-sequestering SER is inaccessible for in vitro investigations of kinetic aspects of the active Ca-uptake mechanism. As a feasible alternative, the present study demonstrates that the rate of ATP-dependent Ca uptake into the SER can be measured microphotometrically in

a few permeabilized single cells. Leech photoreceptor cells are very suitable for these measurements because their Ca^{2+}-sequestering SER is extensive (43, 46), and they lack shielding pigments that would disturb microphotometric recordings.

The intracellularly located SER can be exposed to externally applied media after the plasmalemmal permeability barrier has been broken down by treatment with saponin. The specific mode of action of the plant glycosid saponin has been discussed in several recent reports (see e.g. 4, 13, 31, 43, 46).

The formation of light-microscopically visible Ca-oxalate precipitates within the SER, as a product of its ATP-dependent Ca uptake, is a prerequisite for the microphotometric recording of the birefringence signal. The action of oxalate in facilitating and maintaining active Ca uptake into SER preparations has been investigated and discussed in several previous studies (see e.g. 2, 20, 29, 30, 47).

In brief, Ca-oxalate precipitates can form only in SER cisternae in which the product of the activities of Ca^{2+} and $oxalate^{2-}$ is raised beyond the Ca-oxalate solubility product ($K_{SP} = 2 \times 10^{-8}$ M^2, reference 2). Since precipitation of Ca-oxalate occurs in the SER only, but not in the loading media, Ca^{2+} is accumulated into the SER as a free ion to a concentration higher than in the superfusate. Given a sufficiently high permeability of the SER membrane to oxalate ions, the accumulated Ca^{2+} will be trapped in the SER as soon as K_{SP} has been reached or exceeded and Ca^{2+} is precipitated as Ca-oxalate. The precipitates will grow with continuing active Ca^{2+} entry. Although the SER cisternae become heavily loaded, the outwardly directed Ca^{2+}-gradient will not increase further but will stay at a constant value. This value is set by the apparent K_{SP} within the SER, the intracisternal oxalate activity, and the free Ca^{2+} concentration in the loading medium. The fixed and relatively low intracisternal free Ca^{2+} concentration ($[Ca^{2+}]_{SER}$) prevents the back-inhibition of the pump (29). Thus, the addition of oxalate to the loading medium prolongs the period over which the rate of Ca-oxalate formation closely matches the rate of Ca^{2+} entry (29).

In the present study, Ca-oxalate serves as a birefringent tracer for the accumulated Ca^{2+}. The rate of Ca-oxalate formation in the SER is measured microphotometrically and used as a measure of the Ca-uptake rate. With a similar technique, Sorenson et al. (40) followed the uptake of Ca^{2+} into chemically skinned skeletal muscle fibers by monitoring the changes in light scattering accompanying the active Ca oxalate formation in the SR.

In previous studies on active Ca uptake by SR from skeletal (see e.g., references 29 and 40) and smooth muscle (see e.g., reference 16) it was found that the effect of oxalate on Ca uptake rate saturates at 5–10 mM oxalate. In the saponin-permeabilized leech photoreceptor cells, 5 mM oxalate led to the formation of detectable Ca-oxalate precipitates, localized in the SER (46). However, even at the highest oxalate concentrations used (90 mM), the Ca-uptake rate did not saturate completely (Fig. 8). The nonsaturating behavior of the oxalate dependency might be explained in one or both of two ways: (*a*) Because $[Ca^{2+}]_{SER}$ is decreased with increasing oxalate concentration, the outwardly directed Ca^{2+}-gradient is also decreased. If the SER membrane in the saponin-permeabilized cells is leaky for Ca ions, a small Ca^{2+}-gradient will reduce passive Ca^{2+} loss before the accumulated Ca^{2+} is precipitated as Ca-oxalate. (*b*) If the activity of the Ca pump is governed by $[Ca^{2+}]_{SER}$, any back-inhibition of the pump would be minimized with decreasing $[Ca^{2+}]_{SER}$.

Requirements for higher oxalate concentrations (>10 mM) to produce Ca-oxalate deposits in the SER (SR) were also reported for fragmented cardiac muscle cells (14), cryostat-sectioned cardiac and skeletal muscle cells (27), as well as for a microsomal fraction obtained from rabbit brains (42).

Methodologically, in the present study the use of higher oxalate concentrations did not present any problems. A spontaneous precipitation of Ca-oxalate did not occur in any of the media used.

The requirement for ATP in producing Ca-oxalate precipitates in the SER of the visual cells excludes the possibility that the precipitate formation is the result of some spontaneous, unspecific and/or passive process. This is also supported by the ability to influence the rate of Ca-oxalate formation pharmacologically.

In two preceding papers (43, 46) it was shown electron microscopically that the Ca-oxalate precipitates formed only in the SER. Mitochondrial precipitates were observed extremely rarely. Thus, there was no need to add inhibitors of mitochondrial Ca uptake to the loading media to suppress a possible contribution of mitochondrial Ca uptake to the rise of the optical signal.

Properties of the Ca-sequestering SER: Comparative Aspects

The Ca-sequestering SER in leech photoreceptors shares important functional properties with the SR of skeletal muscle cells (e. g., references 28, 41) and Ca-sequestering microsomal preparations isolated from a variety of nonmuscle cells (see especially references 4, 5, and also 12, 32, 39, 42).

Most notably, the high affinity to Ca^{2+} ions ($K_{M,Ca} \cong 0.4$ μM) is a common property of leech photoreceptor SER, skeletal muscle SR, as well as the Ca-sequestering SER (30) in presynaptic nerve terminals (4, 5). Further similarities between the Ca^{2+}-accumulating SER from these cell types include the apparently high permeability of the SER membrane to oxalate ions, the requirement for MgATP as an energy-supplying substrate for the active Ca uptake, and the inhibitory action of the SH reagent mersalyl and the local anesthetic tetracaine (see reference 4).

The affinity for MgATP ($K_{M,MgATP} \cong 0.8$ mM) of the Ca-uptake mechanism in the photoreceptor SER is lower than in skeletal muscle SR and the SER in presynaptic nerve terminals ($K_{M,MgATP} \cong 10$–20 μM; see reference 5) but higher than in rat liver microsomes ($K_{M,MgATP} \cong 1.8$ mM; see reference 32).

The effect of monovalent cations (Na^+, Li^+) on the active Ca uptake which is normally measured in K^+ rich solutions is very similar to the effects reported by Blaustein et al. (4) for experiments with SER in presynaptic nerve terminals.

Physiological Significance of the Ca^{2+}-sequestering SER

The dependence of active Ca uptake on the Ca^{2+} concentration in the loading medium shows that the Ca uptake mechanism of the SER in leech photoreceptors has a high affinity to Ca^{2+} ions and functions at physiological Ca^{2+} concentrations. The physiological significance of this Ca^{2+}-accumulating organelle is further strengthened by its proximity to the photoreceptive membrane of the cell, where it forms an elaborate cisternal network in the submicrovillar region (43, 46). Less elaborate, but also well developed, are Ca^{2+}-sequestering sub-

surface cisternae associated with the nonreceptive plasma membrane areas of the cell (43). These two prominent high-affinity Ca^{2+}-buffering SER elements thus possess a strategic position relative to the cell periphery where stimulus-induced changes of Ca_{in}^{2+} (6, 8, 9, 26) most probably take place.

For the following arguments it is important to know that the photoreceptor cells of *Balanus* (23), *Limulus* (11) and the honey bee (34) also contain an elaborate SER which has a topography similar to that of the SER of leech photoreceptors (43, 46). The perirhabdomal (submicrovillar) SER in the photoreceptors of the honey bee have also been shown to contain a high Ca content (34).

If the photoreceptive (microvillar) membrane is the main site where Ca^{2+} enters the cell upon illumination, there will be an increase of Ca_{in}^{2+} in the submicrovillar region. It can be predicted from the kinetic data that an increase of Ca_{in}^{2+} above $\sim 5 \times 10^{-8}$ M will activate the pump of the Ca^{2+}-sequestering SER to decrease Ca_{in}^{2+} to the prestimulus concentration. Thus, the stimulus-induced changes of Ca_{in}^{2+} remain largely confined to the periphery of the cell. This would at least partially protect the mitochondria-rich subregion of the cell against large fluctuations of the cytosolic free Ca^{2+} concentration (see e.g. references 5, 10, and 31 for discussions of this aspect).

This function of Ca-sequestering SER elements might be one reason for striking discrepancies that have been reported for the magnitude of the light-induced changes of Ca_{in}^{2+}. Brown and Rydqvist (6) measured in *Balanus* photoreceptors with Ca^{2+}-sensitive microelectrodes a resting intracellular Ca^{2+} concentration of $\sim 7.5 \times 10^{-8}$ M. This value is approximately doubled by illumination. Measurements of the light-induced changes of Ca_{in}^{2+} with the Ca^{2+} indicator dye arsenazo III, however, indicate that Ca_{in}^{2+} rises upon illumination to $10^{-5} - 10^{-4}$ M (6, 8). This discrepancy might be caused by the methodological problem that both Ca^{2+} monitoring methods detect Ca_{in}^{2+} changes in different cytosolic subregions: while the Ca^{2+}-sensitive microelectrode makes a "point measurement" probably in the cellular core which is partially shielded from the subplasmalemmal regions by Ca^{2+}-sequestering SER, the diffusible dye arsenazo III might also detect Ca_{in}^{2+} changes in the immediate vicinity of the plasmalemma.

Recently, Harary and Brown (19) reported that in *Limulus* ventral photoreceptors the light-induced rise of Ca_{in}^{2+} is in fact confined to one region of the cell immediately after the onset of illumination and only at later times begins to diffuse throughout the cell.

The experiment in which the effects of monovalent cations (K^+, Na^+, Li^+) on the rate of Ca uptake into the SER have been investigated might help to understand the desensitizing effect of sodium injections on photoreceptors of *Limulus* (25) and the honey bee (1). This effect might be partially due to a sodium-induced increase of Ca_{in}^{2+}. This could be caused by a slight inhibition of the Ca uptake mechanism of the SER (as observed in this study), or by a sodium-induced release of Ca^{2+} from intracellular stores as supposed by Baumann et al. (1), or by a combined effect.

There can be little doubt that a main function of Ca^{2+}-sequestering SER in invertebrate photoreceptor cells is that of an effective Ca^{2+} sink close to the plasmalemma, especially to its photoreceptive part. It remains to be elucidated whether there is also a light-induced release of Ca^{2+} from this organelle.

The author wishes to thank Mrs. E. Picca for excellent technical assistance and Professor J. B. Walther and R. Paulsen for helpful comments during the preparation of this manuscript. I am especially grateful to Dipl.-Math. H. P. Huber who wrote the computer program and to Professor R. Rüdel who lent out the photomultiplier. I would also like to thank Dr. R. Douglas for correcting the English text.

This work was supported by a grant (Wa 463/1-1) from the Deutsche Forschungsgemeinschaft.

Received for publication 8 October 1981, and in revised form 25 January 1982.

REFERENCES

1. Bader, C. R., F. Baumann, and D. Bertrand. 1976. Role of intracellular calcium and sodium in light adaptation in the retina of the honeybee drone (*Apis mellifera*, L.). *J. Gen. Physiol.* 67:475–491
2. Beil, F.-U., D. von Chak, W. Hasselbach, and H.-H. Weber. 1977. Competition between oxalate and phosphate during active calcium accumulation by sarcoplasmic vesicles. *Z. Naturforsch.* 32:281–287
3. Bennet, H. S. 1950. The microscopical investigation of biological materials with polarized light. *In:* McClung's Handbook of Microscopical Techniques, 3rd Ed. R. M. Jones, editor. Hoeber, New York. 591–672.
4. Blaustein, M. P., R. W. Ratzlaff, N. C. Kendrick, and E. S. Schweitzer. 1978. Calcium buffering in presynaptic nerve terminals. I. Evidence for involvement of a nonmitochondrial ATP-dependent sequestration mechanism. *J. Gen. Physiol.* 72:15–41
5. Blaustein, M. P., R. W. Ratzlaff, and E. S. Schweitzer. 1978. Calcium buffering in presynaptic nerve terminals. II. Kinetic properties of the nonmitochondrial Ca sequestration mechanism. *J. Gen. Physiol.* 72:43–66
6. Brown, H. Mack, and B. Rydqvist. 1980. Changes of intracellular Ca^{2+} in Balanus photoreceptors probed with Ca^{2+} microelectrodes and arsenazo III. *Proc. Int. Union Phys. Sci.* 14:339 (Abstr.).
7. Brown, J. E. 1977. Calcium ion, a putative intracellular messenger for light-adaptation in *Limulus* ventral photoreceptors. *Biophys. Struct. Mech.* 3:141–143
8. Brown, J. E., P. K. Brown, and L. H. Pinto. 1977. Detection of light-induced changes of intracellular ionized calcium concentration in *Limulus* ventral photoreceptors using arsenazo III. *J. Physiol.* 267:299–320
9. Brown, J. E., and J. R. Blinks. 1974. Changes in intracellular free calcium concentration during illumination of invertebrate photoreceptors: detection with aequorin. *J. Gen. Physiol.* 64:643–665
10. Carafoli, E., and M. Crompton. 1978. The regulation of intracellular calcium. *In:* Current Topics in Membranes and Transport. Vol. 10. F. Bronner and A. Kleinzeller, editors. Academic Press. New York. 151.
11. Clark, A. W., R. Millecchia, and A. Mauro. 1969. The ventral photoreceptor cells of *Limulus*. I. The microanatomy. *J. Gen. Physiol.* 54:289–309
12. DeMeis, L., B. M. Rubin-Altschul, and R. D. Machado. 1970. Comparative data of Ca transport in brain and skeletal muscle microsomes. *J. Biol. Chem.* 245:1883–1889
13. Endo, M., and M. Iino. 1980. Specific perforation of muscle cell membranes with preserved SR functions by saponin treatment. *J. Muscle Res. Cell Motil.* 1:89–100
14. Fabiato, A., and F. Fabiato. 1978. Calcium-induced release of calcium from the sarcoplasmic reticulum of skinned cells from adult human, dog, cat, rabbit, rat, and frog hearts and from fetal and new-born rat ventricles. *Annu. N. Y. Acad. Sci.* 307:491–522
15. Fein, A., and J. Sherwood Charlton. 1977. A quantitative comparison of the effects of intracellular calcium injections and light adaptation on the photoresponse of *Limulus* ventral photoreceptors. *J. Gen. Physiol.* 70:591–600
16. Ford, G. D., and M. L. Hess. 1975. Calcium-accumulating properties of subcellular fractions of bovine vascular smooth muscle. *Circ. Res.* 37:580–587
17. Grossman, Y., J. A. Schmidt, and D. L. Alkon. 1981. Calcium-dependent potassium conductance in the photoresponse of a nudibranch mollusk. *Comp. Biochem. Physiol.* 68:487–494
18. Hanani, M., and C. Shaw. 1977. A potassium contribution to the response of the barnacle photoreceptor. *J. Physiol.* 270:151–163
19. Harari, H. H., and J. E. Brown. 1981. Rapid-scanning photometric examination of intracellular Arsenazo III in *Limulus* ventral photoreceptors. *Biophys. J.* 33(*Abstr.*):205 *a*
20. Hasselbach, W., and M. Makinose. 1961. Die calciumpumpe der "erschlaffungsgrana" des muskels und ihre abhängigkeit von der ATP-spaltung. *Biochem. Z.* 333:518–528
21. Johnson, P. N., and G. Inesi. 1969. The effect of methylxanthines and local anesthetics on fragmented sarcoplasmic reticulum. *J. Pharmacol. Exp. Ther.* 169:308–314
22. Kirschfeld, K., and K. Vogt. 1981. Calcium ions and pigment migration in fly photoreceptors. *Naturwissenschaften.* 67:516
23. Krebs, W., and B. Schaten. 1976. The lateral photoreceptor of the barnacle, *Balanus eburneus*. Quantitative morphology and fine structure. *Cell Tissue Res.* 168:193–207
24. Lisman, J. E., and J. E. Brown. 1975. Effect of intracellular injection of calcium buffers on light adaptation in *Limulus* ventral photoreceptors. *J. Gen. Physiol.* 66:489–506
25. Lisman, J. E., and J. E. Brown. 1972. The effects of intracellular iontophoretic injection of calcium and sodium ions on the light response of *Limulus* ventral photoreceptors. *J. Gen. Physiol.* 59:701–719
26. Maaz, G., and H. Stieve. 1980. The correlation of the receptor potential with the light induced transient increase in intracellular calcium concentration measured by absorption change of arsenazo III injected into *Limulus* ventral nerve photoreceptor cells. *Biophys. Struct. Mech.* 6:191–208
27. Mabuchi, K., and F. A. Sréter. 1978. Use of cryostat sections for measurements of Ca^{2+} uptake by sarcoplasmic reticulum. *Anal. Biochem.* 86:733–742
28. MacLennan, D. H., and P. C. Holland. 1975. Calcium transport in sarcoplasmic reticulum. *Annu. Rev. Biophys. Bioeng.* 4:377–404
29. Makinose, M., and W. Hasselbach. 1965. Der einfluß von oxalat auf den calcium-transport isolierter vesikel des sarkoplasmatischen reticulum. *Biochem. Z.* 343:360–382
30. Martonosi, A., and R. Feretos. 1964. Sarcoplasmic reticulum. I. The uptake of Ca^{2+} by sarcoplasmic reticulum fragments. *J. Biol. Chem.* 239:648–658
31. McGraw, C. F., A. V. Somlyo, and M. P. Blaustein. 1980. Localization of calcium in presynaptic nerve terminals. *J. Cell Biol.* 85:288–241
32. Moore, L., T. Chen, H. R. Knapp, Jr., and E. J. Landon. 1975. Energy-dependent calcium sequestration activity in rat liver microsomes. *J. Biol. Chem.* 250:4562–4568
33. Nanninga, L. B. 1961. The association constants of the complexes of adenosine triphosphate with magnesium, calcium, strontium, and barium ions. *Biochim. Biophys. Acta.* 54:330
34. Perrelet, A., and C. R. Bader. 1978. Morphological evidence for calcium stores in

photoreceptors of the honeybee drone retina. *J. Ultrastruct. Res.* 63:237–243
35. Pinto, L. H., and J. E. Brown. 1977. Intracellular recordings from photoreceptors of the squid (*Loligo pealii*). *J. Comp. Physiol.* 122:241–250
36. Portzehl, H., P. C. Caldwell, and J. Rüegg. 1964. The dependence of contraction and relaxation of muscle fibers from the crab *Maia squinado* on the internal calcium concentration. *Biochim. Biophys. Acta.* 79:581–591
37. Reuben, J. P., P. W. Brandt, M. Berman, and H. Grundfest. 1971. Regulation of tension in the skinned crayfish muscle fiber. I. Contraction and relaxation in the absence of Ca (pCa > 9). *J. Gen. Physiol.* 57:385–407
38. Schmidt, J. A., and A. Fein. 1979. Effects of calcium-blocking agents and phosphodiesterase inhibitors on voltage-dependent conductances in *Limulus* photoreceptors. *Brain Res.* 176:369–374
39. Sehlin, J. 1976. Calcium uptake by subcellular fractions of pancreatic islets. *Biochem. J.* 156:63–69
40. Sorenson, M. M., J. P. Reuben, A. B. Eastwood, M. Orentlicher, and G. M. Katz. 1980. Functional heterogeneity of the sarcoplasmic reticulum within sarcomeres of skinned muscle fibers. *J. Membrane Biol.* 53:1–17
41. Tada, M., T. Yamamoto, and Y. Tonomura. 1978. Molecular mechanism of active calcium transport by sarcoplasmic reticulum. *Physiol. Rev.* 58:1–79
42. Trotta, E. E., and L. de Meis. 1975. ATP-dependent calcium accumulation in brain microsomes. Enhancement by phosphate and oxalate. *Biochim. Biophys. Acta.* 394:239–247
43. Walz, B. 1982. Ca^{2+}-sequestering smooth endoplasmic reticulum in an invertebrate photoreceptor. I. Intracellular topography as revealed by OsFeCN staining and *in situ* Ca accumulation. *J. Cell Biol.* 93:839–848
44. Walz, B. 1981. Intracellular topography and functional properties of Ca^{2+}-sequestering smooth endoplasmic reticulum in an invertebrate photoreceptor. *Eur. J. Cell Biol.* 24(2, Pt. 2):25 *a* (Abstr.).
45. Walz, B. 1981. Ca^{++} uptake by smooth ER in leech photoreceptors: microphotometric measurements and electron microscopy. Invest. Ophthal. ARVO Spr. Abs. Suppl. April 1981, p 215
46. Walz, B. 1979. Subcellular calcium localization and ATP-dependent Ca^{2+} uptake by smooth endoplasmic reticulum in an invertebrate photoreceptor cell. An ultrastructural, cytochemical, and x-ray microanalytical study. *Eur. J. Cell Biol.* 20:83–91
47. Weber, A., R. Herz, and I. Reiss. 1966. Study of the kinetics of calcium transport by isolated fragmented sarcoplasmic reticulum. *Biochem. Z.* 345:329–369